



Persistent dopamine functions of neurons derived from embryonic stem cells in a rodent model of Parkinson's disease.

| | |
|-------------------------------|--|
| Journal: | <i>Stem Cells</i> |
| Manuscript ID: | draft |
| Manuscript Type: | Original Research |
| Date Submitted by the Author: | n/a |
| Complete List of Authors: | <p>Rodriguez-Gomez, Jose; National Institutes of Health. National Institute of Neurological Disorders and Stroke, Laboratory of Molecular Biology; Hospital Universitario Virgen del Rocio, Laboratorio de Investigaciones Biomedicas</p> <p>Lu, Jian-Qiang; National Institutes of Health. National Institute of Mental Health., Molecular Imaging Branch.; Foothills Medical Centre, Department of Pathology & Lab Medicine</p> <p>Velasco, Ivan; National Institutes of Health. National Institute of Neurological Disorders and Stroke., Laboratory of Molecular Biology.; Universidad Nacional Autónoma de México, Instituto de Fisiología Celular</p> <p>Rivera, Seth; Brookhaven National Laboratory, Department of Medicine. Behavioral Neuropharmacology & Neuroimaging Laboratory</p> <p>Zoghbi, Sami; National Institutes of Health. National Institute of Mental Health., Molecular Imaging Branch.</p> <p>Liow, Jeh-San; National Institutes of Health. National Institute of Mental Health., Molecular Imaging Branch.</p> <p>Musachio, John; National Institutes of Health. National Institute of Mental Health., Molecular Imaging Branch.</p> <p>Chin, Frederick; National Institutes of Health. National Institute of Mental Health., Molecular Imaging Branch.</p> <p>Toyama, Hiroshi; National Institutes of Health. National Institute of Mental Health., Molecular Imaging Branch.</p> <p>Seidel, Jurgen; National Institutes of Health., Clinical Center Green, Michael; National Institutes of Health., Clinical Center</p> <p>Thanos, Panayotis; Brookhaven National Laboratory, Department of Medicine. Behavioral Neuropharmacology & Neuroimaging Laboratory; National Institutes of Health. National Institute on Alcohol Abuse and Alcoholism, Laboratory of Neuroimaging</p> <p>Ichise, Masanori; National Institutes of Health. National Institute of Mental Health., Molecular Imaging Branch.</p> <p>Pike, Victor; National Institutes of Health. National Institute of Mental Health., Molecular Imaging Branch.</p> <p>McKay, Ronald; Natl Inst of Neurological Disorders, Laboratory of Molecular Biology</p> |

1
2
3
4
5
6
7
8
9
10
11
12
13
14
15
16
17
18
19
20
21
22
23
24
25
26
27
28
29
30
31
32
33
34
35
36
37
38
39
40
41
42
43
44
45
46
47
48
49
50
51
52
53
54
55
56
57
58
59
60

| | |
|-----------|--|
| Keywords: | Parkinson-s disease, Embryonic stem cell, Long-term engraftment, microdialysis, positron emission tomography, dopamine transporter |
| | |

powered by ScholarOne
Manuscript Central™

For Peer Review

1
2
3
4
5
6
7
8
9
10
11
12
13
14
15
16
17
18
19
20
21
22
23
24
25
26
27
28
29
30
31
32
33
34
35
36
37
38
39
40
41
42
43
44
45
46
47
48
49
50
51
52
53
54
55
56
57
58
59
60

Persistent dopamine functions of neurons derived from embryonic stem cells in a rodent model of Parkinson's disease.

Running title: Function of ES cell grafts in Parkinsonian rats

Jose A. Rodríguez-Gómez^{*1,6}, Jian-Qiang Lu^{*2,7}, Iván Velasco^{1,8}, Seth Rivera⁴, Sami S. Zoghbi², Jieih-San Liow², John L. Musachio², Frederick T. Chin², Hiroshi Toyama², Jurgen Seidel³, Michael V. Green³, Panayotis K. Thanos^{4,5}, Masanori Ichise², Victor W. Pike², Robert B. Innis^{†2}, Ron D.G. McKay^{†1}

¹Laboratory of Molecular Biology, NINDS Porter Neuroscience Research Center;

²Molecular Imaging Branch, NIMH; ³Clinical Center, National Institutes of Health, Bethesda, MD 20892; ⁴Medical Department, Brookhaven National Laboratory, Upton, New York 11973-5000; ⁵Laboratory of Neuroimaging, National Institute on Alcohol Abuse and Alcoholism, National Institutes of Health, Bethesda, MD 20892.

Current addresses: ⁶Laboratorio de Investigaciones Biomédicas, Hospital Universitario Virgen del Rocío, Seville, 41013, Spain; ⁷Department of Pathology & Lab Medicine, Foothills Medical Centre, Calgary, AB T2N 2T9, Canada; ⁸Instituto de Fisiología Celular, Universidad Nacional Autónoma de México, Mexico City 04510, Mexico.

**, †Contributed equally to this work as first* or last† authors.*

Correspondence should be addressed to Ron McKay, Laboratory of Molecular Biology, National Institute of Neurological Disorders and Stroke, 35 Convent Drive, Building 35, Room 3A-201, MSC 3703. Bethesda, MD 20892. E-mail: mckayr@ninds.nih.gov

1
2
3
4
5
6
7
8
9
10
11
12
13
14
15
16
17
18
19
20
21
22
23
24
25
26
27
28
29
30
31
32
33
34
35
36
37
38
39
40
41
42
43
44
45
46
47
48
49
50
51
52
53
54
55
56
57
58
59
60

Six figures and one table.

Key words: Parkinson’s disease, embryonic stem cell, transplantation, microdialysis, positron emission tomography, dopamine transporter

For Peer Review

Abstract

Differentiation of dopamine (DA) neurons that might be used in Parkinson's disease is one of the best examples of the potential value of embryonic stem (ES) cells, but little is known of long-term function of the grafted neurons. Here we show that after transplantation into the striatum of 6-hydroxy-dopamine (6-OHDA)-lesioned animals, neurons derived from mouse ES cells survived for over 32 weeks, maintained midbrain markers, and had sustained behavioral effects. Microdialysis in grafted animals showed DA release was induced by depolarization and pharmacological stimulants. Positron emission tomography (PET) quantified the emergence of dopamine transporters (DAT) in the striatum with grafted ES cells. The lesion caused a unilateral increase in the number of postsynaptic DA D₂ receptors, which was normalized with ES cell transplantation. These data demonstrate that ES-cell derived neurons show functions *in vivo* associated with DA synthesis, storage, and release for long periods after implantation and support continued interest in ES cells as a source of functional DA neurons.

Introduction

Parkinson's disease is a neurodegenerative disorder characterized by the progressive loss of dopaminergic neurons in the substantia nigra. Transplantation of dopamine (DA) neuron precursors into the striatum of patients suggests that neuronal replacement may be a feasible treatment [1]. However, two recent double-blind transplantation trials with Parkinson's disease patients raise concerns about both the therapeutic benefit and disabling consequences of fetal cell grafting [2, 3, 4]. Further development of a transplantation therapy requires a consistent source of DA neurons and clear evidence of DA function in pre-clinical models.

Human tissue is currently used as a source of DA neurons, but this supply is limited and difficult to develop as a routine technology. In principle, the controlled proliferation and differentiation of fetal precursor cells is an attractive source for cell-based therapies. Precursor cells in the fetal midbrain can expand in tissue culture and generate DA neurons that provide behavioral recovery in Parkinsonian animals [5, 6]. However, these cells only proliferate for short periods in culture and do not provide sufficient numbers of DA neurons. Embryonic stem (ES) cells may overcome the limitations of fetal donor tissue by offering both extensive cell proliferation and controlled differentiation to DA neurons [7, 8]. DA neurons derived from mouse and non-human primate ES cells integrate and provide behavioral recovery in several experimental animal models [9, 10, 11, 12, 13, 14]. More recent work shows that human ES cells also differentiate into DA neurons, but the function of these cells has not been fully established [15, 16, 17, 18, 19]. Indeed, little evidence exists that

1
2
3 neurons derived from ES cells from any species survive with DA function for long
4
5 periods after grafting to the adult brain.
6
7
8
9

10 In the present study, the stability of DA neurons derived from ES cells was
11 analyzed *in vivo* with a particular focus on their dopaminergic properties. Microdialysis
12 was used to directly measure DA and DA breakdown products generated by grafted
13 cells. Positron emission tomography (PET) imaging was used to measure both a
14 presynaptic and postsynaptic marker: the dopamine transporter (DAT) and the DA D₂
15 receptor, respectively. Furthermore, a method for the precise quantification of specific
16 binding of DAT ligand was developed. We found that neurons derived from mouse ES
17 cells survive *in vivo* for several months, express presynaptic dopaminergic features and
18 influence postsynaptic DA response mechanisms in striatal host cells.
19
20
21
22
23
24
25
26
27
28
29
30
31
32
33
34
35
36
37
38
39
40
41
42
43
44
45
46
47
48
49
50
51
52
53
54
55
56
57
58
59
60

Materials and Methods

In vitro differentiation of ES cells to DA neurons. Mouse R1 ES cells were induced to differentiate into neurons with DA phenotype using a previously established five-stage protocol [8]. This method is based on the formation of embryoid bodies (EBs) and further selection, proliferation and differentiation of neural progenitors into postmitotic neurons.

Immunocytochemistry and histological procedures. Cultured cells were fixed for immunostaining either at the proliferation or differentiation stages in 4% paraformaldehyde/0.15% picric acid/phosphate buffered saline (PBS). For analysis of transplanted animals, rats were deeply anesthetized with sodium pentobarbital and transcardially perfused with isotonic saline, followed by the fixative solution used for cultured cells. The brains were dissected, postfixed for 4 h, cryoprotected with 30% sucrose for 24 - 48 h, and then frozen in isopentane cooled by solid CO₂. Cryostat sections (25 μm) were stained as floating slices. Fixed cells or brain slices were incubated with the primary antibodies overnight at 4 °C. The following antibodies were used: mouse anti-engrailed-1 (En-1) 1:10 (Developmental Studies Hybridoma Bank, Iowa City, IA); rabbit anti-Lmx1b, 1:5000 (gift from C. Birchmeier); goat anti-Foxa2, 1:50 (Santa Cruz Biotechnology, Santa Cruz, CA); rabbit anti-tyrosine hydroxylase (TH), 1:400 (PelFreeze Biologicals, Rogers, AR); mouse anti-TH, 1:1000 (Sigma); mouse anti-Hu 1:50 (Molecular Probes, Eugene, OR); rabbit anti-Ptx3, 1:1000 (gift from J. P. Burbach); rabbit anti-RALDH1, 1:100 (gift from G. Duester); mouse anti-calbindin, 1:3000 (Sigma) and rat anti-DA transporter (DAT), 1:5000 (Chemicon). Appropriate fluorescent-tagged secondary antibodies (Molecular Probes) and 4'-6-

1
2
3 diamidino-2-phenylindole (DAPI) nuclear counterstain were used for visualization. We
4
5 used a Zeiss 510 confocal microscope to make optical sections of the cells after
6
7 staining. Cells were counted *in vitro* by systematic sampling of 20 X fields across the
8
9 length and breadth of each well. Twenty fields were counted per well, and 4 wells were
10
11 analyzed in three independent cultures. TH+ somata in grafted animals were counted on
12
13 every third section on 20 X fields (n=5). Only stained cells with visible dendrites were
14
15 considered positive neurons.
16
17
18
19

20
21
22 *Grafting and implantation of microdialysis probe holders.* All experimental procedures
23
24 conformed to the Guide for Care and Use of Laboratory Animals and were approved by
25
26 the NINDS Animal Care and Use Committee. Taconic Farms (Germantown, NY)
27
28 provided adult female Sprague-Dawley rats (170-190 g) with unilateral 6-hydroxy-
29
30 dopamine (6-OHDA) lesions. A total of 8 μg 6-OHDA was infused in 4 μL over 4 min
31
32 into the nigrostriatal pathway. After arrival at NIH, the animals were housed in a
33
34 temperature-controlled environment with a 12-h light-dark cycle for at least one week
35
36 before the experiments began. Standard rat chow and distilled water were supplied *ad*
37
38 *libitum*. ES cell-derived neurons were trypsinized at day 2-3 of differentiation stage and
39
40 re-suspended at 80,000 viable cells per μL after vital trypan blue exclusion counting.
41
42 Animals were anesthetized with isoflurane, and two grafts were implanted by injecting
43
44 3 μL of the cell suspension into the lesioned striatum at the following coordinates:
45
46 anteroposterior (AP) = + 0.3 mm (first graft), - 0.3 mm (second graft), mediolateral
47
48 (ML) = -3.0 mm and dorsoventral (DV) = - 6.0 mm relative to bregma and the skull,
49
50 with the tooth bar set at 0.0 mm. We deposited 0.5 μL of cell suspension (grafted) or
51
52 medium without cells (sham), waited 1 min, advanced the syringe 0.5 mm dorsally, and
53
54 injected 0.5 μL . This procedure was repeated 5 times to deposit cells over a distance of
55
56
57
58
59
60

1
2
3 2.5 mm in the dorsoventral axis. Implanted cells totaled 480,000 per animal – i.e., a
4
5 number that we previously showed to promote behavioral recovery [10]. We then
6
7 implanted microdialysis probe holders bilaterally with stereotaxic coordinates AP = 0.0
8
9 mm, LM = \pm 3.0 mm, and DV = – 2.0 mm and secured them with acrylic cement. Small
10
11 screws were introduced into the skull, taking care of not damaging the brain, to provide
12
13 support to the cement, which covered the probe holders and closed the wound
14
15 completely. Sham and grafted subjects were immunosuppressed with cyclosporine A
16
17 during the length of the experiment (Neoral, Novartis, 10 mg/kg/day, intraperitoneally,
18
19 i.p.), starting 24 h before grafting [10].
20
21
22
23
24
25
26

27 *Rotational behavior.* Stereotypic rotational behavior was assessed (Rota Count-8,
28
29 Columbus Instruments, Columbus, OH) for 70 min after injection of amphetamine (2.5
30
31 mg/kg, subcutaneous; Sigma). Asymmetry scores are expressed as net 360° turns per
32
33 min. Rotations were measured before and after cell grafting. Animals with stable scores
34
35 of >6 ipsilateral turns per min after lesion were used further.
36
37
38
39
40

41 *Microdialysis experiments.* Twelve weeks after implantation surgery, 4-mm long
42
43 microdialysis probes (CMA, Solna, Sweden) were introduced in both striata to measure
44
45 extracellular monoamine concentrations. *In vitro* recovery experiments with the dialysis
46
47 membranes had values of 18%, 15%, 17% and 11% for DA, DOPAC, HVA and 5-
48
49 HIAA, respectively. The probes were perfused with artificial cerebrospinal fluid at 2
50
51 μ L/min, and fractions were collected every 10 min. Monoamines were stabilized by
52
53 adding a solution containing 0.1 N perchloric acid, 0.02% EDTA and 1% ethanol, kept
54
55 at 4 °C, frozen in dry ice, and then stored at -80 °C until measurement. Extracellular DA
56
57 increases were obtained through chemical depolarization (isosmotic solution with 100
58
59
60

1
2
3 mM potassium chloride), DA uptake blockade (50 μ M nomifensine), and reversal of
4
5 DA uptake (30 μ M amphetamine). Dialysate samples were quantified for monoamine
6
7 content by high-performance liquid chromatography (HPLC) with electrochemical
8
9 detection (GBC, Hubbardston, MA). No recovery correction was performed.
10
11

12
13
14
15 *[¹⁸F]FECNT Imaging.* PET DAT scans were performed at NIH 24 - 28 weeks
16
17 following ES-cell transplantation. Animals were anesthetized with 1.5-2.0 % isoflurane,
18
19 and body temperature was maintained at 36.5 - 37.0 °C. The ATLAS (Advanced
20
21 Technology Laboratory Animal Scanner) PET device has an aperture of 11.8 cm
22
23 diameter and a 2 cm axial field-of-view [20]. Each animal was positioned prone in the
24
25 PET scanner so that striatum and cerebellum were within the field of view. Images were
26
27 reconstructed by 3D ordered subset expectation maximization algorithm (3 iterations),
28
29 achieving a 1.65 mm full-width at half maximum resolution at the center [21, 22, 23].
30
31 The reconstructed voxel size was 0.56 x 0.56 x 1.125 mm. Coronal images were created
32
33 for subsequent data analysis. Image data were not corrected for attenuation or scatter,
34
35 which was relatively minor because of the rat's small head.
36
37
38
39
40
41
42

43
44 [¹⁸F]FECNT was prepared as previously described [24, 25] with the principal
45
46 modification being that the intermediate 1-[¹⁸F]fluoro-2-tosyloxyethane was purified by
47
48 semi-preparative HPLC (acetonitrile/water gradient; Waters RP18 XTerra column 7.8
49
50 mm x 300 mm) and isolated in acetonitrile via solid phase extraction. The ¹⁸F-labeled
51
52 alkylating agent was then reacted with 0.75 mg of CNT (2 β -carbomethoxy-3- β -(4-
53
54 chlorophenyl)nortropine). The alkylation reaction was performed in an open, heated
55
56 vessel (110 °C; 10 min), and the acetonitrile solvent (originally ~1.2 mL) was
57
58 concentrated to less than 0.1 mL by a low flow of helium gas (10 mL/min) that was
59
60

1
2
3 bubbled into the solution. A second HPLC purification on the semi-preparative column
4 using an acetonitrile/10 mM NH₃ gradient afforded [¹⁸F]FECNT of high chemical and
5 radiochemical purity. Specific activity at the time of injection ranged from 42.6
6
7
8 GBq/μmol (1.2 Ci/μmol) to 235.6 GBq/μmol (6.4 Ci/μmol), with a mean ± S.D. of
9
10
11
12
13
14
15
16
17
18
19
20
21
22
23
24
25
26
27
28
29
30
31
32
33
34
35
36
37
38
39
40
41
42
43
44
45
46
47
48
49
50
51
52
53
54
55
56
57
58
59
60

126.5 ± 75.7 GBq/μmol (3.4 ± 2.0 Ci/μmol).

To establish the methodology with [¹⁸F]FECNT, we used three groups of naïve rats that underwent one of the following procedures: (1) Five animals received a bolus injection of 15-34 MBq/h [¹⁸F]FECNT and were scanned for 120 ~ 180 min using 24 or 27 frames of increasing duration (6 x 20 s, 5 x 1 min, 4 x 2 min, 3 x 5 min, 3 x 10 min, 3-6 x 20 min). (2) Five animals received 32-63 MBq/h [¹⁸F]FECNT as a constant infusion for 240 min (30 frames: 6 x 20 s, 5 x 1 min, 4 x 2 min, 3 x 5 min, 3 x 10 min, 9 x 20 min), during which serial blood samples (25 μL) were collected every 20 min via a femoral artery catheter. (3) Four animals were injected subcutaneously with methylphenidate (10 mg/kg) at the midpoint of constant infusion that was the junction of two 100-min acquisition (46 frames: 6 x 20 s, 5 x 1 min, 4 x 2 min, 3 x 5 min, 3 x 10 min, 2 x 20 min and 6 x 20 s, 5 x 1 min, 4 x 2 min, 3 x 5 min, 3 x 10 min, 2 x 20 min).

For 6-OHDA-lesioned rats, [¹⁸F]FECNT was administered as a constant infusion of 26 - 37 MBq/h and a volume of 0.45 - 0.75 mL/h. Rats with 6-OHDA lesions were uniformly scanned for 240 min, and a blood sample (50 μL) was collected from a lateral saphenous vein between 180 and 190 min after starting the infusion. Blood samples were centrifuged at 1,800 g for 3 min. Plasma samples (50 - 80 μL) were mixed with 300 μL of acetonitrile containing UV-standard of FECNT followed by the addition of 100 μL of distilled water and mixed well. Radioactivity in this mixture was measured to

1
2
3 calculate the concentration of total radioactivity (i.e., parent tracer plus metabolites) in
4 plasma. Deproteinized plasma samples were then centrifuged at 9,400 g for 4 min to
5
6 remove the denatured proteins. To correct plasma parent concentrations for the presence
7
8 of radiometabolites, the supernatant was analyzed with reversed phase HPLC on
9
10 Novapak C₁₈ column(Waters Corp., Milford, MA) with a radial compression module
11
12 RCM-100 and a mobile phase of MeOH:H₂O:Et₃N (80:19.9:0.1) at a flow rate of 1.5
13
14 mL/min. Recovery was always more than 90 %. All radioactivity measurements were
15
16 decay-corrected to the time of injection (T_{1/2} = 110 min). We found that the
17
18 concentrations of parent [¹⁸F]FECNT in plasma were similar in femoral arterial and
19
20 saphenous venous samples (unpublished data).
21
22
23
24
25
26
27
28

29
30 We recently reported that a radiolabeled metabolite of [¹⁸F]FECNT accumulates
31
32 in rat brain and confounds the ability to quantify DAT [26]. The radiometabolite results
33
34 from N-dealkylation and is an ¹⁸F-labeled two-carbon fragment, which rapidly converts
35
36 from fluoroethanol to fluoroacetylaldehyde to fluoroacetic acid. The latter is charged and
37
38 accumulates in brain. As described in Results, we developed a method of constant
39
40 infusion of [¹⁸F]FECNT for the current study to provide reliable quantitation of the
41
42 density of DAT in rodent brain. In brief, after constant infusion of the radiotracer, the
43
44 concentration of parent radiotracer in plasma as well as specific binding in brain
45
46 (defined as activity in striatum minus that in cerebellum) becomes stable. The ratio of
47
48 specific binding in brain to the plasma radiotracer concentration is distribution volume,
49
50 which is proportional to density (B_{max}) of DAT [27].
51
52
53
54
55
56

57
58 [¹¹C]Raclopride Imaging. After DAT imaging at NIH, the animals were transported to
59
60 Brookhaven National Laboratory for PET DA D₂ receptor scans that were performed 30

1
2
3 – 32 weeks after ES-cell transplantation. Rats were anesthetized intraperitoneally with
4 ketamine (100 mg/kg) / xylazine (10 mg/kg) and placed in a stereotaxic head holder in a
5 prone position on the Concorde microPET R4 scanner bed (Concorde Microsystems,
6
7
8
9
10
11 Knoxville, TN). Animals were then injected via tail vein catheter with a mean dose of
12
13 1.56 nmol/kg [^{11}C]raclopride (6.5 ± 3.0 MBq for grafted and 5.5 ± 2.8 MBq for sham;
14
15 specific radioactivity was 81 – 170 GBq/ μmol and injected volumes were <500 μL).
16
17 [^{11}C]raclopride binding in the microPET R4 has been previously demonstrated as a
18
19 reproducible and suitable method to study the D_2 receptor availability in the rodent
20
21 brain [28, 29]. The microPET R4 scanner has a 12-cm animal port with an image field
22
23 of view of ~ 11.5 cm. Total acquisition time was 60 min (24 frames: 6 x 10 s, 3 x 20 s, 8
24
25 x 1 min, 4 x 5 min, 3 x 10 min), and data acquired in fully dimensional mode with
26
27 maximum axial acceptance angle (± 28 deg). Images were reconstructed using FORE
28
29 rebinning [30], followed by 2-dimensional filtered back-projection with a ramp cutoff at
30
31 Nyquist frequency. Using the rat stereotaxic atlas [31] and the Hardarian glands as
32
33 reference points, the coronal planes of the striatum and cerebellum were identified as
34
35 slices 6 and 16, respectively, caudal to the Hardarian glands (slice thickness 1.2 mm)
36
37
38
39
40
41 [32, 30, 31, 28] .
42
43
44
45

46 *Image Analysis.* To define brain anatomic structures, MRI images were acquired using a
47
48 7T horizontal small animal MRI system (Bruker Biospin, Billerica, MA) with a spin
49
50 echo sequence (TR = 1500 ms, TE = 10.29 ms) from naïve rats with a similar body
51
52 weight. PET images were analyzed with PMOD v2.4 (pixel-wise modeling computer
53
54 software, PMOD Group, Zurich, Switzerland). Coregistration (FSL Library, Oxford) of
55
56 PET with the MRI images facilitated the placement of regions of interest over striatum
57
58 and cerebellum. In the images of both [^{18}F]FECNT and [^{11}C]raclopride, the right
59
60

1
2
3 striatum (non-lesioned side) was typically delineated on 3-4 different coronal planes,
4
5 from which a central single image plane was chosen for analyzing regions of interest so
6
7 as to minimize axial partial-volume effects [29]. The regions of interest (~22-28 mm³)
8
9 followed the anatomical contour of the right striatum in the MR image (Fig. 5D) and/or
10
11 the stereotaxic rat brain atlas [31]. To be symmetrical, each template of the right
12
13 striatum was copied and pasted/mirrored to the left striatum, with slight manual
14
15 adjustment of placement according to anatomical references.
16
17
18

19
20
21
22 DAT binding of [¹⁸F]FECNT was quantified as an equilibrium distribution
23
24 volume that was calculated as the stable level of specific binding in the brain divided by
25
26 the stable plasma concentration of radiotracer [33, 27]. Specific binding was defined as
27
28 the uptake in striatum minus that in cerebellum. D₂ receptor binding of [¹¹C]raclopride
29
30 was analyzed with a multilinear reference tissue model [23].
31
32
33

34
35
36 *Statistical analysis.* Each group of data passed a normality test before it was analyzed
37
38 with parametric statistics. An unpaired two-tailed student's *t*-test was used to assess
39
40 group differences; a paired two-tailed student's *t*-test was performed to make
41
42 comparisons between bilateral striata. Significance was considered when $p < 0.05$ or $p <$
43
44 0.01 .
45
46
47
48
49
50
51
52
53
54
55
56
57
58
59
60

Results

Expression of midbrain specific markers in precursors and differentiated neurons.

Mouse ES cells were differentiated following a five-stage protocol that allows efficient differentiation of CNS precursors in EBs [34] and modified to generate DA neurons [8, 10]. Markers of regional identity such as En1, Pax2 and Otx2 showed that this method generated proliferating neural precursors with mid- and hindbrain phenotypes. The mid/hindbrain boundary region and the mesencephalic floor plate act as organizing centers regulating neuronal differentiation by the production of fibroblast growth factor (FGF)-8 and sonic hedgehog (Shh) [35]. The differentiation of ES cells into DA precursors was regulated by these signals and, thus, provided additional evidence that the *in vitro* generated cells mimic aspects of normal midbrain development. The five stages of the differentiation protocol are: (1) proliferating ES cells; (2) differentiating ES cell aggregates, EBs; (3) nestin-positive cells that migrate from the EBs under minimal growth conditions; (4) a proliferative step when these CNS precursor cells expand in number and midbrain specification is promoted by FGF-8 and Shh; and (5) a differentiation step when neurons are efficiently generated. At step 4, many cells expressing the transcription factors En1, Lmx1b and Foxa2 were observed (Fig. 1A, B). Approximately 40 % of the total cells expressed En1, a gene that has an important role in midbrain progenitors (Fig. 1B) [36]. 8 % of the cells co-expressed all three genes (Fig. 1B). Cell autonomous expression of Lmx1b and Foxa2 are thought to be essential for the differentiation of DA neurons and the floor plate [37, 38]. In a parallel study focused on normal development, it is proposed that Foxa2-positive floor plate cells

1
2
3 directly generate the Lmx1b-positive DA neurons (Kittappa, Wang and McKay;
4 unpublished data). The co-expression of Foxa2 and Lmx1b suggests that this precursor
5 cell type is also present in ES derived En1-positive populations (Fig. 1A, B). The
6 presence of En1+, Foxa2-, Lmx1b+ cells was not expected from *in vivo* studies and
7 might reflect short term regulation of the expression of the Foxa2 protein rather than a
8 cell of a different fate [39]. These data show that up to 30 % of the cells express
9 combinations of genes found in the ventral midbrain DA neuron precursor population.
10
11
12
13
14
15
16
17
18
19
20
21

22 In the final step, this protocol generates neurons from neural precursors. After
23 10 days of differentiation in stage 5, the gene expression profile of the differentiated
24 neurons was assessed. All tyrosine hydroxylase positive (TH+) cells expressed the
25 neuronal marker Hu (Fig. 1C). Approximately 11 ± 1 % of Hu+ cells were also TH+.
26 This result is consistent with previous data suggesting that without genetic manipulation
27 a small proportion of neurons acquire the dopaminergic fate [8,10]. Foxa2 is also
28 expressed in mature DA neurons (Kittappa, Wang and McKay; unpublished data) and
29 30 ± 3 % of the Foxa2+ neurons generated *in vitro* co-expressed TH (Fig. 1C). En1 was
30 co-expressed in all TH+ neurons, as it has been observed in differentiated adult TH+
31 neurons, and in DA neurons generated in our previous study (Fig. 1C) [36, 10]. Ptx3 is a
32 transcription factor specifically expressed in DA neurons [40]. Ptx3 was coexpressed in
33 the great majority of TH+ neurons (99 ± 1 %; Fig. 1C). Calbindin is expressed in the
34 dorsal part of substantia nigra *pars compacta* of rats [41]. Only a small proportion ($1 \pm$
35 0.1 %) of the TH+ neurons co-expressed calbindin *in vitro* (Fig. 1C). RALDH1 is also
36 a specific marker of DA neurons in the ventral part of substantia nigra *pars compacta*
37 [42, 43]. In ES cells-derived neurons, 42 ± 1 % of TH+ cells express RALDH1 (Fig.
38 1C). The DAT is critical to appropriate neurotransmitter recycling [44, 45]. DAT was
39
40
41
42
43
44
45
46
47
48
49
50
51
52
53
54
55
56
57
58
59
60

1
2
3 expressed by TH⁺ cells after longer times of *in vitro* differentiation (20 days in stage 5,
4 Fig. 1C). These data suggest that TH⁺ neurons derived from ES cells have patterns of
5 gene expression characteristic of dopaminergic cells in the ventral midbrain.
6
7
8
9

10
11
12 The technical difficulty of grafting *ex vivo* generated cells demands simple
13 procedures. As a consequence, in this study the mouse ES cells were not genetically
14 manipulated prior to the five-stage differentiation protocol nor were optimal
15 differentiation conditions for DA neurons developed. The results show that a small
16 proportion of neurons are TH⁺, but the expression of *En1*, *Foxa2*, *Ptx3* and *RALDH1*
17 suggest that many cells have the potential to generate the ventral DA cell type that is
18 preferentially lost in Parkinson's disease [46]. The data also suggest that other types of
19 neurons are present. A clear example is the small proportion of neurons that are
20 apparently of a hindbrain serotonin⁺ type as we have previously noted [10]. This
21 analysis of gene expression raised the question of whether the transplanted population
22 of cells had sufficient DA neurons of the ventral *pars compacta* type to be effective in
23 the lesioned striatum.
24
25
26
27
28
29
30
31
32
33
34
35
36
37
38
39
40
41
42

43 **Long-term sustained behavioral recovery induced by DA reinnervation in the** 44 **striatal terminal field.** 45 46 47 48 49

50
51 Neurons derived from the same batch as characterized above were grafted into the
52 striatum of 6-OHDA lesioned animals. The behavior of transplanted animals was
53 measured for up to 32 weeks after the surgery as a first measure of long-term survival of
54 functional grafted neurons. Four weeks after implantation into the dorsal striatum, the
55 grafts caused an abrupt change of amphetamine-induced rotational behavior (Fig. 2A).
56
57
58
59
60

1
2
3 The kinetics of the behavioral recovery was comparable to that in our previous study
4 [10]. In contrast, a gradual change in behavior has been reported when no specific *in*
5 *vitro* steps were used to control ES cell differentiation prior to grafting [9]. With the
6 exception of a slight change at 12 weeks after grafting that is coincident with the
7 placement of a microdialysis probe and a possible disruption of dopaminergic terminals,
8 this behavioral change was stable for 32 weeks.
9
10
11
12
13
14
15
16
17
18
19

20 The murine cells in the host brains were identified with M2-mouse specific
21 antibody allowing clear identification of the graft as donor cell derived (data not
22 shown). The grafts project a dense extension of TH-positive processes into the dorso-
23 lateral striatum (Fig. 2B₁). RALDH1 immunostaining identifies projections in a similar
24 distribution to TH in the dorsal striatum (Fig. 2B₃). On the unlesioned side of the brain,
25 RALDH1-positive processes from the DA neurons of the ventral substantia nigra
26 projected to the dorsal lateral striatum, as previously reported (Fig. 2B₄) [42]. At 32
27 weeks, 5385 ± 4638 (mean \pm S.E.M.) TH⁺ cells were found in lesioned striatum of
28 grafted animals. Thus, grafted DA neurons survived in large numbers for 32 weeks,
29 extended strong RALDH1 projection to the dorsolateral striatum and regulated
30 behavior.
31
32
33
34
35
36
37
38
39
40
41
42
43
44
45
46
47
48
49
50
51
52

53 **DA release and monoamine levels in grafted animals.**

54 Microdialysis was used to monitor DA production by the grafted cells. Extracellular
55 monoamine levels were measured simultaneously in the lesioned and non-lesioned
56 striata of sham and grafted animals. Baseline DA levels were elevated on both sides of
57 the brain after grafting, although only in the grafted side reached statistical significance
58
59
60

1
2
3 when comparison was performed against both striata of sham animals (Table 1). In
4
5 contrast to DA itself, the metabolites DOPAC and HVA showed right/left asymmetry.
6
7 Grafting caused a partial restoration of DOPAC and HVA concentrations to about 10 %
8
9 of basal levels (Table 1). The level of the 5-HT metabolite, 5-HIAA, was not altered by
10
11 the lesion to the DA neurons. Meanwhile, a significantly higher level was found in the
12
13 grafted striatum either as a consequence of 5HT-positive neurons in the graft as we have
14
15 shown [10] or due to sprouting of intrinsic serotonergic afferents to striatum induced by
16
17 grafted DA cells [47, 48]. The cause and consequence of bilaterally elevated basal DA
18
19 levels are not known but these data demonstrate that DA and its metabolites are elevated
20
21 in grafted animals.
22
23
24
25
26
27
28

29
30 Extracellular DA levels were measured following three pharmacological
31
32 challenges: (1) depolarization induced by K^+ ions, (2) inhibition of DAT reuptake with
33
34 nomifensine, and (3) administration of amphetamine, which causes the release of DA
35
36 via DAT [49]. Perfusion of isosmotic 100 mM K^+ , 50 μ M nomifensine and 30 μ M
37
38 amphetamine each caused increased DA levels in the non-lesioned striata (Fig. 3A). On
39
40 the lesioned side of sham animals, treatment evoked no change in DA levels
41
42 establishing that the lesions were virtually complete (Fig. 3B). Although DA levels
43
44 were much lower than those in non-lesioned sides, the ES derived neurons responded to
45
46 the three treatments (Fig. 3B). Significant differences were found between sham and
47
48 grafted groups after K^+ -induced depolarization and nomifensine perfusion. In the case
49
50 of amphetamine, the differences did not reach statistical significance, perhaps due to the
51
52 variability of the graft response. In both grafted and non-lesioned sides, DOPAC and
53
54 HVA values underwent important decreases after high potassium and amphetamine
55
56 stimulation as it has been previously shown (Fig. 3C) [50]. These measurements show
57
58
59
60

1
2
3 that transplanted neurons can respond to depolarization and DAT blocking elevating
4
5
6 extracellular DA levels.
7
8
9

10 **[¹⁸F]FECNT imaging showed partial innervation of the lesioned striatum following**
11 **transplantation.**
12
13
14
15
16

17 PET provides a useful non-invasive measure of PD-related changes associated with
18 disease severity [51, 52]. PET imaging has been used to monitor the function of grafted
19 human fetal DA neurons [53, 2, 54, 55]. We developed a method that was independent
20 of cerebral blood flow to measure the abundance of the pre-synaptic DAT in the
21 striatum of rats, using the recently developed radiotracer, 2β-carbomethoxy-3β-(4-
22 chlorophenyl)-8-(2-fluoroethyl)nortropane([¹⁸F]FECNT) [24, 25]. We found that
23
24
25
26
27
28
29
30
31
32
33
34
35
36
37
38
39
40
41
42
43
44
45
46
47
48
49
50
51
52
53
54
55
56
57
58
59
60
[¹⁸F]FECNT generates a radiolabeled two-carbon fragment that accumulates in rat brain
[26]. The effect of this accumulating radiometabolite can be seen following bolus
injection of the radiotracer (Fig. 4A). Radioactivity in cerebellum (which lacks DAT)
was stable after about ~30 min, despite decreasing values in striatum. Radioactivity did
not decline in parallel in striatum and cerebellum because of the accumulation of an
inactive radiometabolite, which represented a higher percentage of total activity in a
nonspecific region like cerebellum than a region with a high DAT density like striatum
[26].

These observations led us to administer [¹⁸F]FECNT as a constant infusion to
achieve steady state levels of parent radiotracer in plasma and equilibrium levels of
receptor binding in brain. Following constant infusion of [¹⁸F]FECNT, radioactivity in
both striatum and cerebellum increased for at least 240 min, but the subtraction (STR-

1
2
3 CBL) of these two signals was stable after ~120 min (Fig. 4B). Specific binding was
4
5 defined as the difference between uptake in striatum and cerebellum. This operationally
6
7 defined specific uptake approximated equilibrium levels by 150 min, since the slopes of
8
9 the fitted lines were only 5.6 ± 4.6 percent per hour, expressed as the mean \pm S.D. of the
10
11 absolute value of slope relative to the value at 150 min ($n = 5$ rats). Injection of
12
13 methylphenidate displaced the specifically bound signal in the striatum to background
14
15 levels providing additional support for the measurement of striatal DAT (Fig. 4C).
16
17 Measurements of arterial blood samples showed plasma [^{18}F]FECNT reached steady-
18
19 state after ~150 min constant infusion (Fig. 4B). Plasma concentrations of the parent
20
21 tracer separated from radiometabolites of individual rats after 150 min of constant
22
23 infusion were fitted linearly. The slopes of these fitted lines were 3.7 ± 5.6 percent per
24
25 hour, expressed as the mean of the absolute values.
26
27
28
29
30
31
32
33

34 Distribution volume is a time- and blood flow-independent parameter that is
35
36 linearly proportional to receptor density [33]. The constant infusion paradigm allowed a
37
38 relatively simple calculation of distribution volume as the mean specific binding (=
39
40 striatum minus cerebellum) from 150 to 210 min divided by the plasma radiotracer
41
42 concentration at 180 - 190 min. The non-lesioned side of the striatum preserved robust
43
44 uptake of the tracer (Fig. 5B), similar to concentrations seen in naive animals (Fig. 5A).
45
46 In contrast, uptake in the lesioned (left) striatum of sham rats, measured as the ratio of
47
48 the lesioned/non-lesioned was reduced by more than 90 % (Fig. 5B, E). The tracer
49
50 uptake was not significantly different in rats receiving the sham procedures (5 ± 3 %)
51
52 compared to no-intervention lesioned animals (4 ± 3 %; Fig. 5E). In contrast, tracer
53
54 uptake was partially restored to 38 ± 17 % of controls in the lesioned striatum after
55
56 grafting (Fig. 5C, E; $p < 0.01$).
57
58
59
60

1
2
3
4
5
6 Specific binding of [^{18}F]FECNT in the lesioned and transplanted striatum (Fig.
7
8 6B) was higher than that of sham animals (Fig. 6A). The distribution volumes of the
9
10 non-lesioned striata were similar in sham and transplanted rats (Fig. 6C). In contrast, the
11
12 distribution volumes of the lesioned striata were significantly increased by
13
14 transplantation (Fig. 6C; 6.71 ± 1.7 vs. 1.15 ± 0.23 , $p < 0.01$; mean \pm S.E.M.).

15
16
17 Distribution volume measurements correct for potential blood flow changes in the
18
19 lesioned striata and show that grafting is associated with long-term expression of DAT.
20
21

22
23
24 **[^{11}C]raclopride imaging indicated normalization of upregulated postsynaptic D₂**
25
26 **receptors.**
27

28
29
30
31
32 PET imaging was also performed with [^{11}C]raclopride, which binds to DA D_{2/3}
33
34 receptors that are present postsynaptically on a subset of striatal medium spiny neurons.
35
36 Treatment with 6-OHDA caused asymmetrical uptake of [^{11}C]raclopride, consistent
37
38 with increased density of D₂ receptors on the side of the lesion [56]. The binding
39
40 potential of [^{11}C]raclopride increased significantly in sham animals when left and right
41
42 striata were compared (2.01 ± 0.28 vs. 1.52 ± 0.34 , $p < 0.01$, $n=4$, mean \pm S.E.M.).
43
44
45 Transplantation normalized D₂ receptors so that the uptake of [^{11}C]raclopride was
46
47 similar in both striata (1.51 ± 0.18 vs 1.50 ± 0.08 , $n=5$, mean \pm S.E.M.) and
48
49 significantly different to left side of sham animals ($p=0.01$; Fig. S1). These data suggest
50
51 that grafted neurons act on host targets cells to correct the super-sensitive increase in
52
53 DA D₂ receptors.
54
55
56
57
58
59
60

Discussion

The use of ES cells as a source of cells for cell therapies has been widely discussed but there are still few experimental systems where this approach has been validated. The derivation of DA neurons from ES cells is one of the best characterized, but even in this case, there are few studies that demonstrate long-term DA functions in grafted animals. To validate ES cells as a suitable source of DA neurons for cell-based therapy in Parkinson's disease, it is important that the neurons maintain DA neurotransmitter functions for prolonged periods. In previous studies we have used electrophysiological and behavioral tools to characterize grafted neurons [10]. However, the electrophysiological approach may be subject to a bias due to the choice of specific neurons for recording and the behavioral measures are indirect tests of neuronal function. In this work we have defined long-term function using assays that directly assess the dopaminergic neurochemical status of grafted animals.

Even though it was not the main focus of this study, it was important to establish the developmental status of the donor cells. The generation of midbrain DA neurons *in vivo* depends on signaling molecules expressed by two organizing centres: the floor plate and the isthmus organizer. FGF-8 and Shh are thought to contribute to the patterning and normal growth of the mid/hindbrain region by regulating expression of transcription factors including engrailed (En1 and En2), Otx2, Gbx2, Pax2, Pax 5, Wnt1, Lmx1b, Foxa2 and Nurr1 [57, 58]. The expression of En1, Lmx1b and Foxa2 characterizes neural progenitor cells generated from ES cells as midbrain cells. After further *in vitro* differentiation, TH + neurons maintained the midbrain phenotype defined by expression of En1, Foxa2, Ptx3 and RALDH1. These results confirm our

1
2
3 previous observations suggesting that *in vivo* developmental processes implicated in the
4 generation of midbrain DA neurons, can be recapitulated by *in vitro* ES cell
5
6 differentiation [10]. In this published study, the mouse ES cells were manipulated by
7
8 gene over-expression which causes a substantial increase in the proportion of DA
9
10 neurons. In the current report, DA neurons were derived from an unmanipulated ES cell
11
12 line and showed changes in behavior and neurochemistry consistent with long term DA
13
14 function.
15
16
17
18
19
20
21

22 The data presented in this study extend our previous work by showing that ES
23 cell-derived DA neurons restored the terminal field in the dorso-lateral striatum and
24 expressed both TH and the midbrain specific marker RALDH1. Retinoic acid
25
26 modulates the level of striatal DA receptors [59, 60, 61] and retinoic receptor mutant
27
28 mice show locomotor defects that can be related to decreased levels of DA receptors
29
30 [62]. The expression of RALDH1 suggests that a proportion of the engrafted DA
31
32 neurons maintain this specific midbrain phenotype following transplantation. Future
33
34 work should more fully characterize the DA neurons in the graft to determine if
35
36 RALDH1-positive cells specifically project to the host.
37
38
39
40
41
42
43
44
45

46 Previous studies show that the effect of grafted primary cells on behavior
47 requires the continued presence of DA neurons [63]. The behavioral data show that
48
49 transplanted animals have altered behavior for seven months. Microdialysis
50
51 experiments shown here suggest that the grafted cells have activity-dependent release
52
53 and a high affinity reuptake system. The elevated baseline DA level compared to the
54
55 partial recovery of stimulated DA release points to autoregulatory mechanisms aimed to
56
57 maintain a normal DA tone despite the partial DA reinnervation achieved in the grafted
58
59
60

1
2
3 striatum. This same phenomenon has been observed in studies of grafted fetal nigral
4 tissue [64, 65, 66]. A candidate to control baseline DA level is the DAT. PET chemistry
5 confirms the expression of the DAT, however post-translational modification can
6 regulate DAT function and may explain the elevated DA level [67, 49].
7
8
9
10
11
12
13
14

15 The PET study supports the utility of DAT imaging as a noninvasive *in vivo*
16 marker for the survival of grafted DA neurons. [¹⁸F]FECNT was previously used in
17 monkeys [24], healthy human subjects, and patients with Parkinson's disease [25], with
18 a high ratio of specific to nonspecific uptake. Contrary to prior reports [24],
19 [¹⁸F]FECNT showed significant accumulation of a polar radiometabolite in rat brain
20 [26]. Because of the time dependent changes in both parent and radiometabolite in brain
21 following a typical bolus injection, no single time point could be *a priori* selected to
22 measure DAT density. For example, Fig. 4A shows that the ratio of striatum to
23 cerebellum continuously declined after about 30 min. At what time does this ratio of
24 specific to nonspecific uptake reflect DAT density? In the current study, we
25 administered [¹⁸F]FECNT as a constant infusion and obtained temporally stable levels
26 of specific binding in striatum as well as the concentration of parent radiotracer in
27 plasma. Distribution volume is the ratio at equilibrium of specific binding in brain to the
28 concentration of drug in plasma, and it is usually regarded as the "gold standard"
29 measurement of *in vivo* receptor density. A simple left/right ratio of activity in lesioned
30 to non-lesioned striata can be used to measure DAT levels (Fig. 5E). However, this
31 ratio can not distinguish whether the lesion or transplant caused any changes to the
32 control side of the brain. Distribution volume can accomplish this comparison, and we
33 report that DAT densities were the same in non-lesioned striata of sham and
34 transplanted animals.
35
36
37
38
39
40
41
42
43
44
45
46
47
48
49
50
51
52
53
54
55
56
57
58
59
60

1
2
3
4
5
6
7
8
9
10
11
12
13
14
15
16
17
18
19
20
21
22
23
24
25
26
27
28
29
30
31
32
33
34
35
36
37
38
39
40
41
42
43
44
45
46
47
48
49
50
51
52
53
54
55
56
57
58
59
60

DAT imaging in rodents has been used to monitor fetal mesencephalic [68] and ES-cell transplantation [9]. The latter study used [^{11}C]CFT, a close chemical analog of [^{18}F]FECNT, and found that at nine weeks after transplantation, the grafted striata of animals with behavioral improvement reached ~75-90 % of DAT levels in the contralateral/non-lesioned side [9]. In this study, we found DAT levels returned to an average of only ~40 % of the control side, with wide variation from ~15 – 55 %. The difference between these data may be caused by cytopathology in the grafted animals in the previous study where blood flow may be altered by the development of a teratoma. In animals grafted with the multi-step protocol no teratomas were found by anatomy and this is also a pre-requisite for the long survival times studied here. Our results show that significant behavioral recovery occurs with ~40% of normal DA terminal innervation, as measured by DAT density in grafted striata at long times after surgery.

The level of DA D₂ receptor expression on striatal neurons was measured by [^{11}C]raclopride PET imaging. Suppression of upregulated postsynaptic D₂ receptors by fetal DA grafts has been shown in Parkinsonian rats [69, 70, 71] and in a PD patient 10 years after fetal transplantation [53]. Our data show that D₂ receptor densities may be restored throughout the striatum despite the partial reinnervation found in the grafted animals. Efficient uptake of DA has been shown in primary grafted DA neurons [65, 72, 73] but other studies report diffusion of extracellular DA that may elevate DA tone over non-innervated areas [74, 75, 76]. The elevated baseline DA we report in grafted animals may account for the normalization of D₂ receptor binding. Recent work shows that DA denervation leads to rapid changes in spine density in striato-pallidal medium

1
2
3 spiny neurons [77]. It will be interesting to analyze other features of postsynaptic
4
5
6 neurons including spine density in grafted animals.
7
8
9

10 In summary, the data presented here show that both pre- and postsynaptic
11
12 functions can be restored by grafting DA neurons derived from ES cells. The immortal
13
14 nature of ES cells will allow genetic manipulations to more precisely define the
15
16 mechanisms regulating the survival and function of DA neurons. This feature will be
17
18 particularly valuable for cell-therapy studies with human ES cells.
19
20
21
22
23
24
25
26
27
28
29
30
31
32
33
34
35
36
37
38
39
40
41
42
43
44
45
46
47
48
49
50
51
52
53
54
55
56
57
58
59
60

1
2
3 **ACKNOWLEDGEMENTS:** We thank Drs. Raja Kittappa and Sachiko Murase for
4 valuable advice and discussion and Jeeva Munasinghe (NINDS) for his technical help
5 with acquiring rat MRI images. We are grateful to Carmen Birchmeier (Max-Delbruck-
6 Center of Molecular Medicine, Berlin, Germany), J. Peter Burbach (Rudolph Magnus
7 Institute of Neuroscience, Utrecht, The Netherlands) and Greg Duester (Burnham
8 Institute, La Jolla, California), for their gifts of antibodies. I.V. was a Pew Latin
9 American Fellow during his stay at NIH and had partial support from DGAPA, UNAM
10 (IN226703). This work was supported in part by the Intramural Program of NIMH
11 (project Z01-MH-002795-04).
12
13
14
15
16
17
18
19
20
21
22
23
24
25
26
27
28
29
30
31
32
33
34
35
36
37
38
39
40
41
42
43
44
45
46
47
48
49
50
51
52
53
54
55
56
57
58
59
60

REFERENCES

1. Lindvall O, Bjorklund A. Cell therapy in Parkinson's disease. *NeuroRx*. Oct 2004;1(4):382-393.
2. Freed CR, Greene PE, Breeze RE, et al. Transplantation of embryonic dopamine neurons for severe Parkinson's disease. *N Engl J Med*. Mar 8 2001;344(10):710-719.
3. Olanow CW, Goetz CG, Kordower JH, et al. A double-blind controlled trial of bilateral fetal nigral transplantation in Parkinson's disease. *Ann Neurol*. Sep 2003;54(3):403-414.
4. Hagell P, Piccini P, Bjorklund A, et al. Dyskinesias following neural transplantation in Parkinson's disease. *Nat Neurosci*. Jul 2002;5(7):627-628.
5. Studer L, Tabar V, McKay RD. Transplantation of expanded mesencephalic precursors leads to recovery in parkinsonian rats. *Nat Neurosci*. Aug 1998;1(4):290-295.
6. Sanchez-Pernaute R, Studer L, Bankiewicz KS et al. In vitro generation and transplantation of precursor-derived human dopamine neurons. *J Neurosci Res*. Aug 15 2001;65(4):284-288.
7. Kawasaki H, Mizuseki K, Nishikawa S, et al. Induction of midbrain dopaminergic neurons from ES cells by stromal cell-derived inducing activity. *Neuron*. Oct 2000;28(1):31-40.
8. Lee SH, Lumelsky N, Studer L, et al. Efficient generation of midbrain and hindbrain neurons from mouse embryonic stem cells. *Nat Biotechnol*. Jun 2000;18(6):675-679.
9. Bjorklund LM, Sanchez-Pernaute R, Chung S, et al. Embryonic stem cells develop into functional dopaminergic neurons after transplantation in a Parkinson rat model. *Proc Natl Acad Sci U S A*. Feb 19 2002;99(4):2344-2349.

- 1
2
3
4
5
6
7
8
9
10
11
12
13
14
15
16
17
18
19
20
21
22
23
24
25
26
27
28
29
30
31
32
33
34
35
36
37
38
39
40
41
42
43
44
45
46
47
48
49
50
51
52
53
54
55
56
57
58
59
60

10. Kim JH, Auerbach JM, Rodriguez-Gomez JA, et al. Dopamine neurons derived from embryonic stem cells function in an animal model of Parkinson's disease. *Nature*. Jul 4 2002;418(6893):50-56.

11. Barberi T, Klivenyi P, Calingasan NY, et al. Neural subtype specification of fertilization and nuclear transfer embryonic stem cells and application in parkinsonian mice. *Nat Biotechnol*. Oct 2003;21(10):1200-1207.

12. Takagi Y, Takahashi J, Saiki H, et al. Dopaminergic neurons generated from monkey embryonic stem cells function in a Parkinson primate model. *J Clin Invest*. Jan 2005;115(1):102-109.

13. Sanchez-Pernaute R, Studer L, Ferrari D, et al. Long-term survival of dopamine neurons derived from parthenogenetic primate embryonic stem cells (Cyno1) after transplantation. *Stem Cells*. Aug 2005;23(7):914-922.

14. Kim DW, Chung S, Hwang M, et al. Stromal cell-derived inducing activity, *nurr1*, and signaling molecules synergistically induce dopaminergic neurons from mouse embryonic stem cells. *Stem Cells*. Mar 2006;24(3):557-567.

15. Zeng X, Cai J, Chen J, et al. Dopaminergic differentiation of human embryonic stem cells. *Stem Cells*. 2004;22(6):925-940.

16. Ben-Hur T, Idelson M, Khaner H, et al. Transplantation of human embryonic stem cell-derived neural progenitors improves behavioral deficit in Parkinsonian rats. *Stem Cells*. 2004;22(7):1246-1255.

17. Park CH, Minn YK, Lee JY, et al. In vitro and in vivo analyses of human embryonic stem cell-derived dopamine neurons. *J Neurochem*. Mar 2005;92(5):1265-1276.

- 1
2
3
4
5
6
7
8
9
10
11
12
13
14
15
16
17
18
19
20
21
22
23
24
25
26
27
28
29
30
31
32
33
34
35
36
37
38
39
40
41
42
43
44
45
46
47
48
49
50
51
52
53
54
55
56
57
58
59
60
18. Yan Y, Yang D, Zarnowska ED, et al. Directed differentiation of dopaminergic neuronal subtypes from human embryonic stem cells. *Stem Cells*. Jun-Jul 2005;23(6):781-790.
19. Brederlau A, Correia AS, Anisimov SV, et al. Transplantation of human embryonic stem cell-derived cells to a rat model of Parkinson's disease: effect of in vitro differentiation on graft survival and teratoma formation. *Stem Cells*. Mar 23 2006.
20. Seidel J, Vaquero J, Green M. Resolution uniformity and sensitivity of the NIH ATLAS small animal PET scanner: comparison to simulated LSO scanners without depth-of-interaction capability. *IEEE Trans Nucl Sci*. 2003; 50:1347-1350.
21. Johnson CA, Seidel J, Vaquero JJ, et al. Exact positioning for OSEM reconstructions on the ATLAS depth-of-interaction small animal scanner. *Mol Imaging Biol*. 2002;4:S22.
22. Liow J, Seidel J, Johnson CA et al. A single slice rebinning/2D exact positioning OSEM reconstruction for the NIH ATLAS small animal PET scanner. *J Nucl Med*. 2003; 44:163P.
23. Ichise M, Liow JS, Lu JQ, et al. Linearized reference tissue parametric imaging methods: application to [¹¹C]DASB positron emission tomography studies of the serotonin transporter in human brain. *J Cereb Blood Flow Metab*. Sep 2003;23(9):1096-1112.
24. Goodman MM, Kilts CD, Keil R, et al. ¹⁸F-labeled FECNT: a selective radioligand for PET imaging of brain dopamine transporters. *Nucl Med Biol*. Jan 2000;27(1):1-12.
25. Davis MR, Votaw JR, Bremner JD, et al. Initial human PET imaging studies with the dopamine transporter ligand ¹⁸F-FECNT. *J Nucl Med*. Jun 2003;44(6):855-861.

- 1
2
3
4
5
6
7
8
9
10
11
12
13
14
15
16
17
18
19
20
21
22
23
24
25
26
27
28
29
30
31
32
33
34
35
36
37
38
39
40
41
42
43
44
45
46
47
48
49
50
51
52
53
54
55
56
57
58
59
60
26. Zoghbi SS, Shetty HU, Ichise M, et al. PET Imaging of the Dopamine Transporter with ^{18}F -FECNT: A Polar Radiometabolite Confounds Brain Radioligand Measurements. *J Nucl Med.* Mar 2006;47(3):520-527.
27. Laruelle M, Abi-Dargham A, al-Tikriti MS, et al. SPECT quantification of [^{123}I]iomazenil binding to benzodiazepine receptors in nonhuman primates: II. Equilibrium analysis of constant infusion experiments and correlation with in vitro parameters. *J Cereb Blood Flow Metab.* May 1994;14(3):453-465.
28. Thanos PK, Taintor NB, Alexoff D, et al. In vivo comparative imaging of dopamine D2 knockout and wild-type mice with ^{11}C -raclopride and microPET. *J Nucl Med.* Nov 2002;43(11):1570-1577.
29. Alexoff DL, Vaska P, Marsteller D, et al. Reproducibility of ^{11}C -raclopride binding in the rat brain measured with the microPET R4: effects of scatter correction and tracer specific activity. *J Nucl Med.* May 2003;44(5):815-822.
30. Matej S, Karp JS, Lewitt RM, et al. Performance of the Fourier rebinning algorithm for PET with large acceptance angles. *Phys Med Biol.* Apr 1998;43(4):787-795.
31. Paxinos G, Watson C. *The Rat Brain in Stereotaxic Coordinates*, 4th ed. New York: Academic Press, 1998.
32. Lammertsma AA, Bench CJ, Hume SP, et al. Comparison of methods for analysis of clinical [^{11}C]raclopride studies. *J Cereb Blood Flow Metab.* Jan 1996;16(1):42-52.
33. Lassen NA. Neuroreceptor quantitation in vivo by the steady-state principle using constant infusion or bolus injection of radioactive tracers. *J Cereb Blood Flow Metab.* Sep 1992;12(5):709-716.

- 1
2
3
4
5
6
7
8
9
10
11
12
13
14
15
16
17
18
19
20
21
22
23
24
25
26
27
28
29
30
31
32
33
34
35
36
37
38
39
40
41
42
43
44
45
46
47
48
49
50
51
52
53
54
55
56
57
58
59
60
34. Okabe S, Forsberg-Nilsson K, Spiro AC, et al. Development of neuronal precursor cells and functional postmitotic neurons from embryonic stem cells in vitro. *Mech Dev.* Sep 1996;59(1):89-102.
35. Ye W, Shimamura K, Rubenstein JL, et al. FGF and Shh signals control dopaminergic and serotonergic cell fate in the anterior neural plate. *Cell.* May 29 1998;93(5):755-766.
36. Simon HH, Saueressig H, Wurst W, et al. Fate of midbrain dopaminergic neurons controlled by the engrailed genes. *J Neurosci.* May 1 2001;21(9):3126-3134.
37. Smidt MP, Asbreuk CH, Cox JJ, et al. A second independent pathway for development of mesencephalic dopaminergic neurons requires Lmx1b. *Nat Neurosci.* Apr 2000;3(4):337-341.
38. Ruiz i Altaba A, Prezioso VR, Darnell JE, et al. Sequential expression of HNF-3 beta and HNF-3 alpha by embryonic organizing centers: the dorsal lip/node, notochord and floor plate. *Mech Dev.* Dec 1993;44(2-3):91-108.
39. Wolfrum C, Besser D, Luca E, et al. Insulin regulates the activity of forkhead transcription factor Hnf-3beta/Foxa-2 by Akt-mediated phosphorylation and nuclear/cytosolic localization. *Proc Natl Acad Sci U S A.* Sep 30 2003;100(20):11624-11629.
40. Smidt MP, van Schaick HS, Lanctot C, et al. A homeodomain gene Ptx3 has highly restricted brain expression in mesencephalic dopaminergic neurons. *Proc Natl Acad Sci U S A.* Nov 25 1997;94(24):13305-13310.
41. Gerfen CR, Herkenham M, Thibault J. The neostriatal mosaic: II. Patch- and matrix-directed mesostriatal dopaminergic and non-dopaminergic systems. *J Neurosci.* Dec 1987;7(12):3915-3934.

- 1
2
3
4
5
6
7
8
9
10
11
12
13
14
15
16
17
18
19
20
21
22
23
24
25
26
27
28
29
30
31
32
33
34
35
36
37
38
39
40
41
42
43
44
45
46
47
48
49
50
51
52
53
54
55
56
57
58
59
60
42. McCaffery P, Drager UC. High levels of a retinoic acid-generating dehydrogenase in the meso-telencephalic dopamine system. *Proc Natl Acad Sci U S A*. Aug 2 1994;91(16):7772-7776.
43. Chung S, Hedlund E, Hwang M, et al. The homeodomain transcription factor Pitx3 facilitates differentiation of mouse embryonic stem cells into AHD2-expressing dopaminergic neurons. *Mol Cell Neurosci*. Feb 2005;28(2):241-252.
44. Amara SG, Kuhar MJ. Neurotransmitter transporters: recent progress. *Annu Rev Neurosci*. 1993;16:73-93.
45. Giros B, Caron MG. Molecular characterization of the dopamine transporter. *Trends Pharmacol Sci*. Feb 1993;14(2):43-49.
46. Jellinger KA. The pathology of Parkinson's disease. *Adv Neurol*. 2001;86:55-72.
47. Takeuchi Y, Sawada T, Blunt S, Jenner P, Marsden CD. Serotonergic sprouting in the neostriatum after intrastriatal transplantation of fetal ventral mesencephalon. *Brain Res*. Jun 14 1991;551(1-2):171-177.
48. Wright AK, Arbuthnott GW, Dunnett SB. Serotonin hyperinnervation after foetal nigra or raphe transplantation in the neostriatum of adult rats. *Neurosci Lett*. Jul 22 1991;128(2):281-284.
49. Khoshbouei H, Sen N, Guptaroy B, et al. N-terminal phosphorylation of the dopamine transporter is required for amphetamine-induced efflux. *PLoS Biol*. Mar 2004;2(3):E78.
50. Zetterstrom T, Sharp T, Collin AK, et al. In vivo measurement of extracellular dopamine and DOPAC in rat striatum after various dopamine-releasing drugs; implications for the origin of extracellular DOPAC. *Eur J Pharmacol*. Apr 13 1988;148(3):327-334.

- 1
2
3
4
5
6
7
8
9
10
11
12
13
14
15
16
17
18
19
20
21
22
23
24
25
26
27
28
29
30
31
32
33
34
35
36
37
38
39
40
41
42
43
44
45
46
47
48
49
50
51
52
53
54
55
56
57
58
59
60
51. Brooks DJ, Frey KA, Marek KL, et al. Assessment of neuroimaging techniques as biomarkers of the progression of Parkinson's disease. *Exp Neurol*. Nov 2003;184 Suppl 1:S68-79.
52. Piccini P, Whone A. Functional brain imaging in the differential diagnosis of Parkinson's disease. *Lancet Neurol*. May 2004;3(5):284-290.
53. Piccini P, Brooks DJ, Bjorklund A, et al. Dopamine release from nigral transplants visualized in vivo in a Parkinson's patient. *Nat Neurosci*. Dec 1999;2(12):1137-1140.
54. Nakamura T, Dhawan V, Chaly T, et al. Blinded positron emission tomography study of dopamine cell implantation for Parkinson's disease. *Ann Neurol*. Aug 2001;50(2):181-187.
55. Bjorklund A, Dunnett SB, Brundin P, et al. Neural transplantation for the treatment of Parkinson's disease. *Lancet Neurol*. Jul 2003;2(7):437-445.
56. Hume SP, Opacka-Juffry J, Myers R, et al. Effect of L-dopa and 6-hydroxydopamine lesioning on [¹¹C]raclopride binding in rat striatum, quantified using PET. *Synapse*. Sep 1995;21(1):45-53.
57. Prakash N, Wurst W. Specification of midbrain territory. *Cell Tissue Res*. Oct 2004;318(1):5-14.
58. Smidt MP, Smits SM, Burbach JP. Molecular mechanisms underlying midbrain dopamine neuron development and function. *Eur J Pharmacol*. Nov 7 2003;480(1-3):75-88.
59. Farooqui SM. Induction of adenylate cyclase sensitive dopamine D2-receptors in retinoic acid induced differentiated human neuroblastoma SHSY-5Y cells. *Life Sci*. 1994;55(24):1887-1893.

- 1
2
3
4
5
6
7
8
9
10
11
12
13
14
15
16
17
18
19
20
21
22
23
24
25
26
27
28
29
30
31
32
33
34
35
36
37
38
39
40
41
42
43
44
45
46
47
48
49
50
51
52
53
54
55
56
57
58
59
60
60. Samad TA, Krezel W, Chambon P, et al. Regulation of dopaminergic pathways by retinoids: activation of the D2 receptor promoter by members of the retinoic acid receptor-retinoid X receptor family. *Proc Natl Acad Sci U S A*. Dec 23 1997;94(26):14349-14354.
61. Valdenaire O, Maus-Moatti M, Vincent JD, et al. Retinoic acid regulates the developmental expression of dopamine D2 receptor in rat striatal primary cultures. *J Neurochem*. Sep 1998;71(3):929-936.
62. Krezel W, Ghyselinck N, Samad TA, et al. Impaired locomotion and dopamine signaling in retinoid receptor mutant mice. *Science*. Feb 6 1998;279(5352):863-867.
63. Dunnett SB, Hernandez TD, Summerfield A, et al. Graft-derived recovery from 6-OHDA lesions: specificity of ventral mesencephalic graft tissues. *Exp Brain Res*. 1988;71(2):411-424.
64. Zetterstrom T, Brundin P, Gage FH, et al. In vivo measurement of spontaneous release and metabolism of dopamine from intrastriatal nigral grafts using intracerebral dialysis. *Brain Res*. Jan 8 1986;362(2):344-349.
65. Strecker RE, Sharp T, Brundin P, et al. Autoregulation of dopamine release and metabolism by intrastriatal nigral grafts as revealed by intracerebral dialysis. *Neuroscience*. Jul 1987;22(1):169-178.
66. Rioux L, Gaudin DP, Bui LK, et al. Correlation of functional recovery after a 6-hydroxydopamine lesion with survival of grafted fetal neurons and release of dopamine in the striatum of the rat. *Neuroscience*. 1991;40(1):123-131.
67. Gnegy ME, Khoshbouei H, Berg KA, et al. Intracellular Ca²⁺ regulates amphetamine-induced dopamine efflux and currents mediated by the human dopamine transporter. *Mol Pharmacol*. Jul 2004;66(1):137-143.

- 1
2
3
4
5
6
7
8
9
10
11
12
13
14
15
16
17
18
19
20
21
22
23
24
25
26
27
28
29
30
31
32
33
34
35
36
37
38
39
40
41
42
43
44
45
46
47
48
49
50
51
52
53
54
55
56
57
58
59
60
68. Inaji M, Yoshizaki T, Okauchi T, et al. In vivo PET measurements with [¹¹C]PE2I to evaluate fetal mesencephalic transplantations to unilateral 6-OHDA-lesioned rats. *Cell Transplant*. 2005;14(9):655-663.
69. Freed WJ, Ko GN, Niehoff DL, et al. Normalization of spiroperidol binding in the denervated rat striatum by homologous grafts of substantia nigra. *Science*. 1983; 222: 937-939.
70. Dawson TM, Dawson VL, Gage FH, et al. Functional recovery of supersensitive dopamine receptors after intrastriatal grafts of fetal substantia nigra. *Exp Neurol*. Mar 1991;111(3):282-292.
71. Rioux L, Gaudin DP, Gagnon C, Di Paolo T, Bedard PJ. Decrease of behavioral and biochemical denervation supersensitivity of rat striatum by nigral transplants. *Neuroscience*. 1991;44(1):75-83.
72. Kalen P, Nilsson OG, Cenci MA, et al. Intracerebral microdialysis as a tool to monitor transmitter release from grafted cholinergic and monoaminergic neurons. *J Neurosci Methods*. Sep 1990;34(1-3):107-115.
73. Wang Y, Wang SD, Lin SZ, et al. Restoration of dopamine overflow and clearance from the 6-hydroxydopamine lesioned rat striatum reinnervated by fetal mesencephalic grafts. *J Pharmacol Exp Ther*. Aug 1994;270(2):814-821.
74. Stromberg I, van Horne C, Bygdeman M, et al. Function of intraventricular human mesencephalic xenografts in immunosuppressed rats: an electrophysiological and neurochemical analysis. *Exp Neurol*. May 1991;112(2):140-152.
75. Cragg SJ, Clarke DJ, Greenfield SA. Real-time dynamics of dopamine released from neuronal transplants in experimental Parkinson's disease. *Exp Neurol*. Jul 2000;164(1):145-153.

1
2
3
4
5
6
7
8
9
10
11
12
13
14
15
16
17
18
19
20
21
22
23
24
25
26
27
28
29
30
31
32
33
34
35
36
37
38
39
40
41
42
43
44
45
46
47
48
49
50
51
52
53
54
55
56
57
58
59
60

76. Stromberg I, Kehr J, Andbjør B, et al. Fetal ventral mesencephalic grafts functionally reduce the dopamine D2 receptor supersensitivity in partially dopamine reinnervated host striatum. *Exp Neurol*. Jul 2000;164(1):154-165.

77. Day M, Wang Z, Ding J, et al. Selective elimination of glutamatergic synapses on striatopallidal neurons in Parkinson disease models. *Nat Neurosci*. Feb 2006;9(2):251-259.

For Peer Review

Table 1. Basal levels of monoamines in perfusates from striatum of sham and grafted animals in lesioned and non-lesioned sides

| | Left lesioned sham | Right non-lesioned | Left lesioned graft | Right non-lesioned |
|-------|--------------------------|--------------------|--------------------------|--------------------|
| DA | 0.76 ± 0.10 | 0.78 ± 0.06 | 2.18 ± 0.16 ^a | 2.05 ± 0.69 |
| DOPAC | 4.26 ± 2.07 ^b | 3105 ± 707 | 233 ± 44 ^a | 2861 ± 734 |
| HVA | 3.87 ± 2.53 ^b | 2283 ± 437 | 240 ± 41 ^a | 2110 ± 421 |
| 5HIAA | 115 ± 35 | 127 ± 38 | 362 ± 78 ^a | 204 ± 55 |

Table 1. Data (mean ± S.E.M.) are averaged from three baseline samples (paired *t*-test; ^a *p* < 0.01 left grafted vs. left and right sham sides; ^b *p* < 0,01 left sham vs. right sham).

Figure legends:

Figure 1. Expression pattern of midbrain related markers by progenitors and differentiated neurons generated from ES cells. **A)** Triple immunocytochemical labelling for En1, Lmx1b and Foxa2 in progenitor cells (day 4, stage 4). **B)** Different cell populations expressing different combinations of genes were observed at this stage. The results are shown as mean \pm S.E.M. **C)** Triple immunocytochemical labelling in differentiated DA neurons (day 10, stage 5). TH⁺ cells express neuronal marker Hu. Foxa2 expression is maintained in differentiated TH⁺ neurons. En1 is expressed in TH⁺ neurons and Ptx3 expression emerges in most of them. A fraction of TH⁺ neurons (42 ± 1 %) expressed RALDH1 protein. Few TH⁺ neurons expressed calbindin, which did not co-localized with Ptx3 gene. Some TH⁺ also co-expressed DAT. Scale = 20 μ m.

Figure 2. Behavioral recovery after ES cell-derived DA neuron grafting, and reinnervation of 6-OHDA lesioned striatum by grafted cells. **A)** Grafting of ES cells caused significant recovery of amphetamine-induced rotational behavior. The results are shown as mean \pm S.E.M. (n = 5; *, P<0.01; #, P < 0.05 by a two-tailed *t*-test, compared with rats receiving the sham treatment). **B)** ES cell-derived DA neurons partially restored TH and RALDH1 immunoreactivity in the lesioned side. TH (green) immunostaining is shown for the grafted (left, **B**₁) and non-lesioned (right, **B**₂) sides and RALDH1 (red) is shown for the grafted (**B**₃) and non-lesioned (**B**₄) sides. DAPI staining is shown in blue color. Scale = 1 mm.

Figure 3. Effect of ES cell-derived DA neuron graft on monoamine levels studied *in vivo* by microdialysis. **A)** Time-course on DA concentration level after 100 mM K⁺

1
2
3 isosmotic medium, 50 μ M nomifensine and 30 μ M amphetamine in the lesioned and
4
5 non-lesioned sides of sham and grafted animals. **B)** Time-course on DA level shown in
6
7 **A** for lesioned sides in grafted and sham groups is shown at bigger scale. **C)** Time-
8
9 course of DOPAC and HVA concentrations for non-lesioned sides of both sham and
10
11 grafted animals and for the lesioned side that received DA neurons. The results are
12
13 shown as mean \pm S.E.M. (n = 5; *, P<0.01; #, P < 0.05 by a two-tailed *t*-test, compared
14
15 with rats receiving the sham treatment).
16
17
18
19
20
21

22 *Figure 4.* Dynamic PET imaging in naïve rats with [18 F]FECNT. **A)** About 30 min after
23
24 bolus injection of [18 F]FECNT (n = 5), activity in cerebellum (CBL) was stable despite
25
26 declining concentrations in striatum (STR). **B)** After ~150 min of constant infusion of
27
28 [18 F]FECNT (n = 5), activities in striatum and cerebellum increased in a linear and
29
30 parallel manner. Specific binding (SPEC) was operationally defined as the difference
31
32 between striatum and cerebellum and, therefore, became stable after ~150 min. The
33
34 plasma concentration of [18 F]FECNT separated from radiometabolites (upper curve)
35
36 after ~170 min of infusion was also obtained. The y-axis on left is for brain
37
38 measurements and is expressed as % of the activity infused per h. The y-axis on right is
39
40 the plasma measurements of the concentration of [18 F]FECNT and is expressed as a
41
42 percentage of the constant infusion: [(plasma [18 F]FECNT dpm/mL)/ activity (mCi)
43
44 infused per hour] * 100. **C)** The difference in TACs between striatum and cerebellum
45
46 was confirmed to be specific binding, since methylphenidate displaced [18 F]FECNT in
47
48 striatum to background levels in cerebellum (n = 4).
49
50
51
52
53
54
55
56
57

58 *Figure 5.* Recovery on DAT binding after grafting of 6-OHDA lesioned animals. **A)** A
59
60 naïve rat showed bilaterally symmetrical uptake of [18 F]FECNT in striata following

1
2
3 constant infusion of the radiotracer. **B)** A hemiparkinsonian rat receiving sham
4 treatment displayed negligible uptake in the lesioned striatum. **C)** ES-cell
5 transplantation partially restored uptake of [^{18}F]FECNT in the lesioned striatum of a
6 hemiparkinsonian rat. **D)** PET and MRI images of hemiparkinsonian rat with ES-cell
7 transplantation into the left striatum were coregistered to define anatomic structures. **E)**
8 ES-cell transplantation increased the ratio of activity in lesioned/non-lesioned striatum
9 determined by PET imaging with [^{18}F]FECNT. The ratio was greatly reduced in
10 hemiparkinsonian rats that had either no intervention (n = 4) or sham treatment (n = 5).
11 This reduced ratio significantly recovered after transplanting ES-cells into the lesioned
12 striatum of hemiparkinsonian rats (n = 5; *, p < 0.01 by a two-tailed *t*-test, compared
13 with rats receiving the sham treatment). The horizontal line on each group shows the
14 mean value.
15
16
17
18
19
20
21
22
23
24
25
26
27
28
29
30
31
32
33

34 *Figure 6.* Recovery on [^{18}F]FECNT specific binding after grafting of 6-OHDA lesioned
35 animals. Time activity curves following constant infusion of [^{18}F]FECNT in rats with
36 **(A)** sham treatment and **(B)** ES cell transplantation. After 120-150 min constant
37 infusion, uptake in both striatum (STR) and cerebellum (CBL) ascended linearly, and
38 specific binding (SPEC = STR - CBL) became stable. Specific binding in the lesioned
39 striatum displayed a minimal level in rats receiving sham treatment **(A)**; n = 5), but
40 increased to approximately 1/3 level of non-lesioned striatum after ES cell
41 transplantation **(B)**; n = 5). The *y*-axis is expressed as % of the activity infused per h.
42 Results are shown as mean \pm S.E.M. **C)** Distribution volumes of [^{18}F]FECNT specific
43 binding in striata of hemiparkinsonian rats. The distribution volumes of the non-
44 lesioned striata were similar in sham (n = 5) and ES cell transplanted (n = 5) animals. In
45 contrast, the distribution volumes of the lesioned striata were significantly higher in
46
47
48
49
50
51
52
53
54
55
56
57
58
59
60

1
2
3 transplanted than in sham animals (6.71 ± 1.7 vs. 1.15 ± 0.23 ; *, $p < 0.01$ by a two-
4
5
6 tailed t -test, compared with rats receiving the sham treatment). The horizontal line on
7
8 each group shows the mean value.
9
10
11
12
13
14
15
16
17
18
19
20
21
22
23
24
25
26
27
28
29
30
31
32
33
34
35
36
37
38
39
40
41
42
43
44
45
46
47
48
49
50
51
52
53
54
55
56
57
58
59
60

For Peer Review

Supplementary figure legend:

Figure S1. Binding potential of [¹¹C]raclopride in striata of hemiparkinsonian rats. The lesioned striata of sham rats (n = 4) showed a significant increase in dopamine D₂ receptor binding compared to the contralateral, non-lesioned side (p < 0.01, paired two-tailed *t*-test). In contrast, receptor binding in transplanted animals (n = 5) was equal on right and left sides and significantly different from left side of sham animals (p=0.01). Results are shown as mean ± S.E.M.

1
2
3
4
5
6
7
8
9
10
11
12
13
14
15
16
17
18
19
20
21
22
23
24
25
26
27
28
29
30
31
32
33
34
35
36
37
38
39
40
41
42
43
44
45
46
47
48
49
50
51
52
53
54
55
56
57
58
59
60

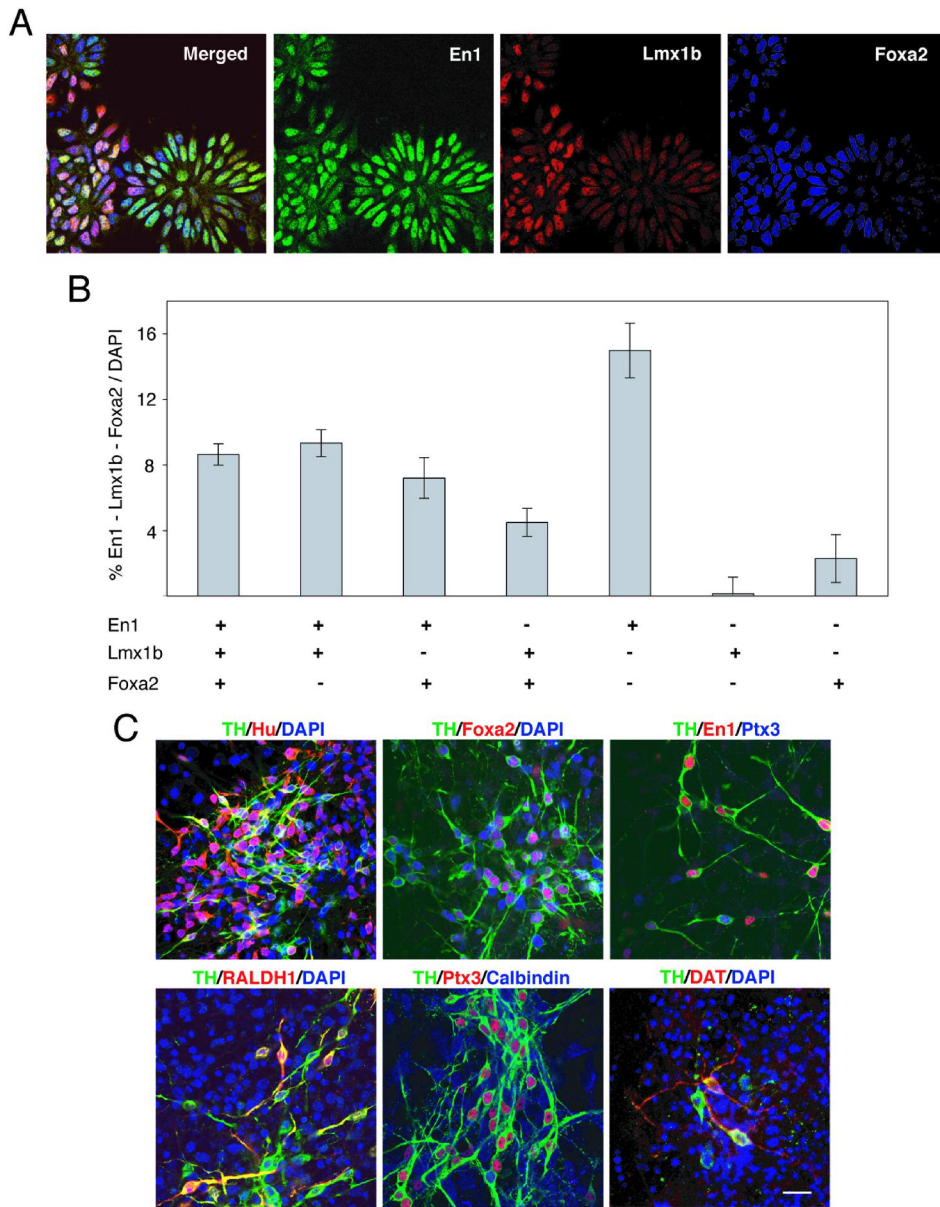


Figure 1

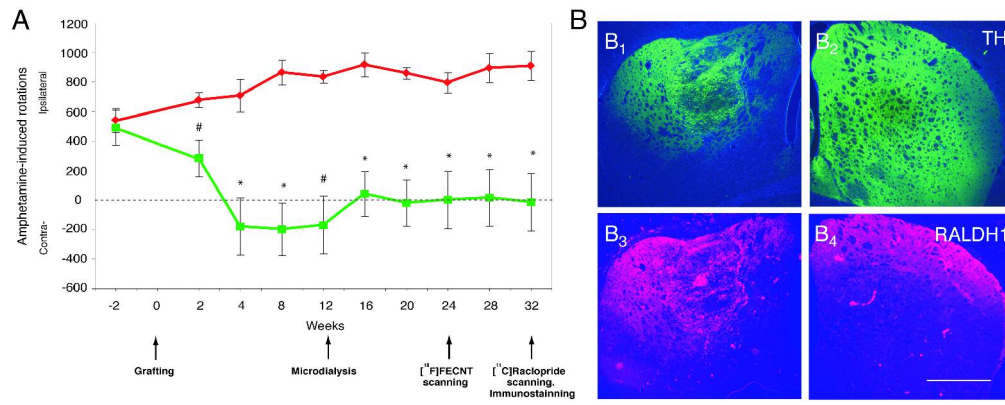


Figure 2

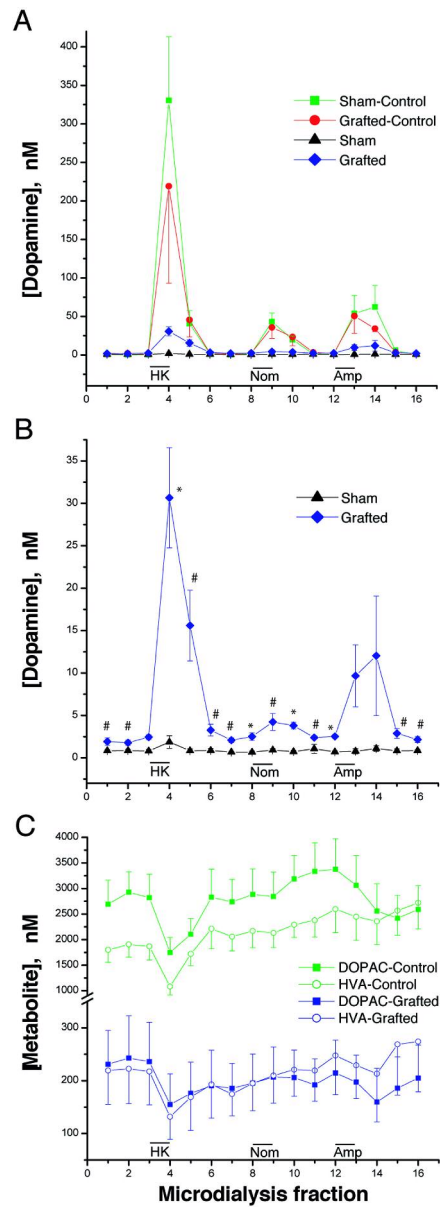


Figure 3

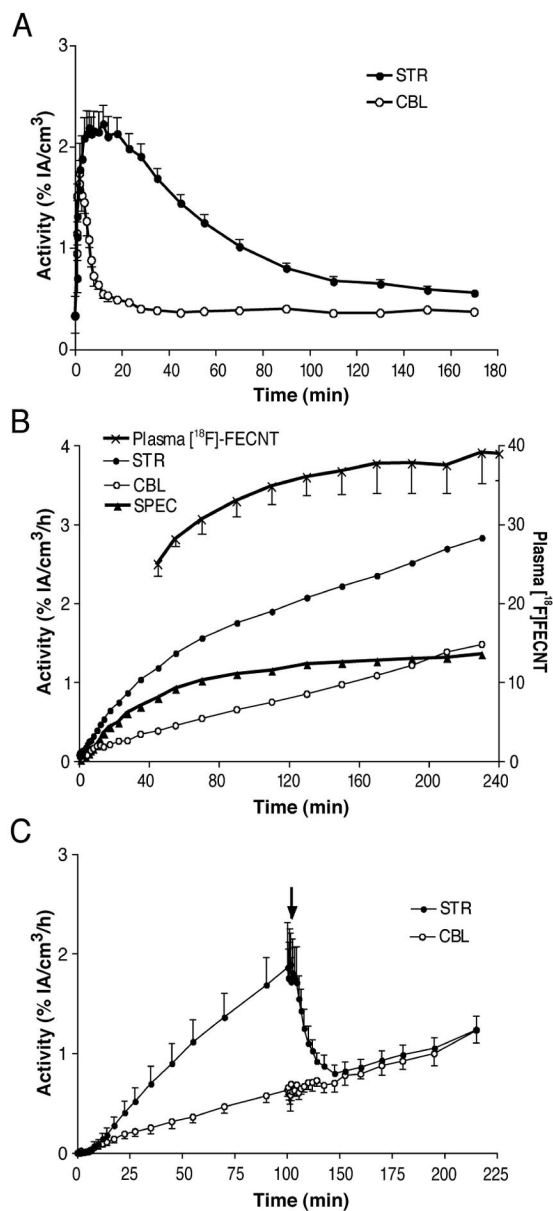


Figure 4

1
2
3
4
5
6
7
8
9
10
11
12
13
14
15
16
17
18
19
20
21
22
23
24
25
26
27
28
29
30
31
32
33
34
35
36
37
38
39
40
41
42
43
44
45
46
47
48
49
50
51
52
53
54
55
56
57
58
59
60

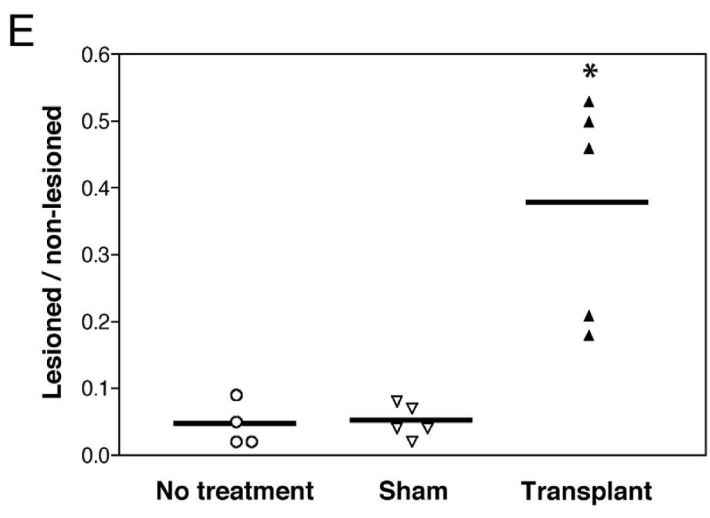
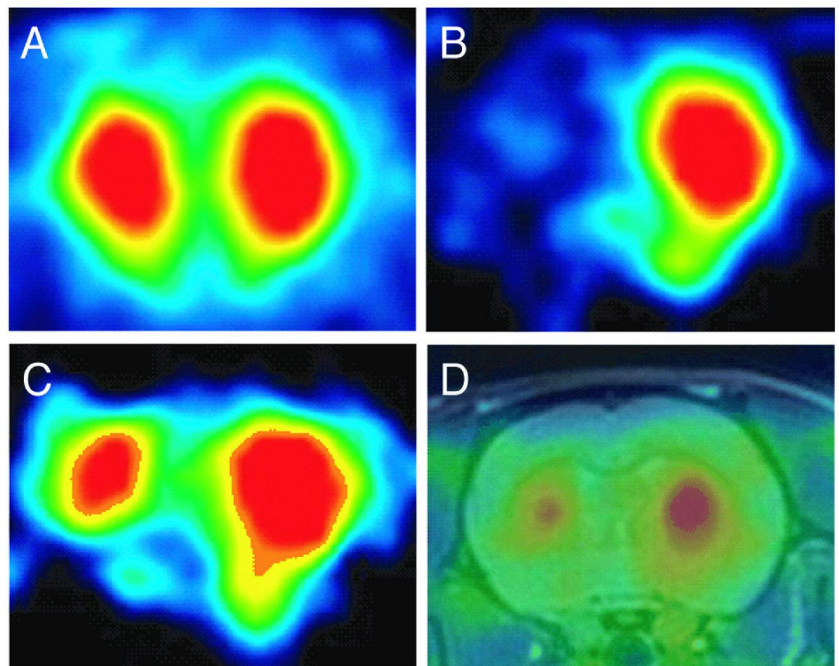


Figure 5

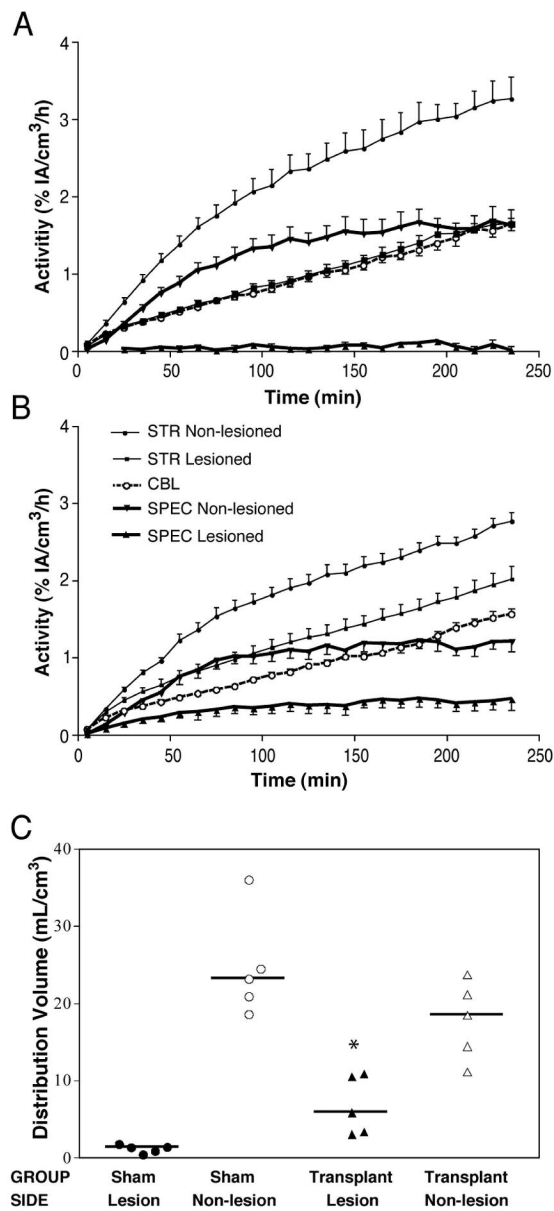


Figure 6

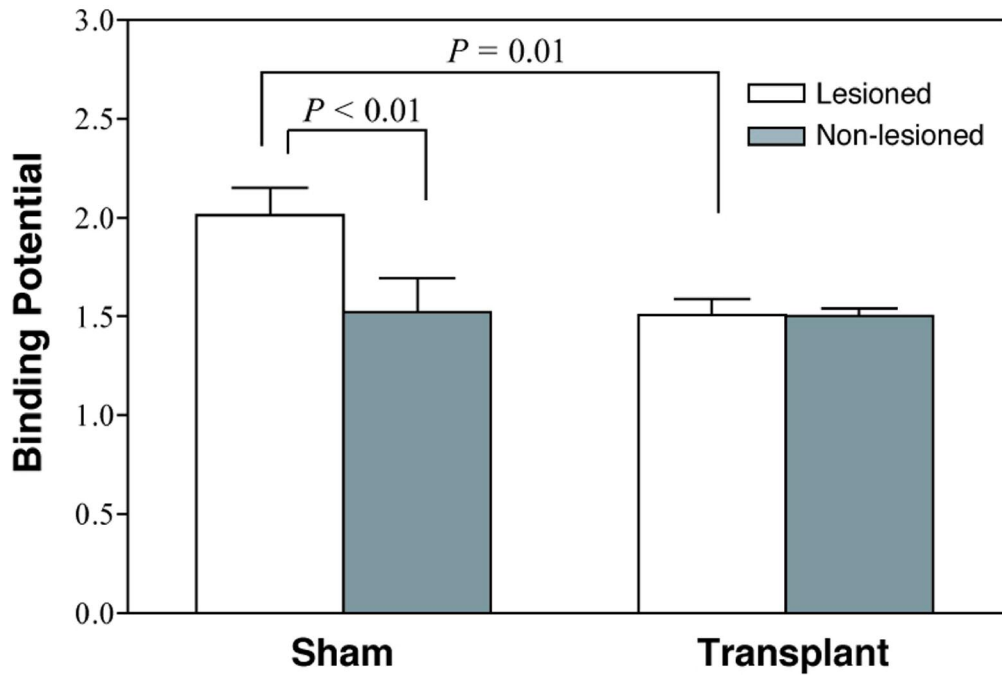


Figure S1

Review